Increased Reactive Oxygen Species Production and Lower Abundance of Complex I Subunits and Carnitine Palmitoyltransferase 1B Protein Despite Normal Mitochondrial Respiration in Insulin-Resistant Human Skeletal Muscle

Natalie Lefort,[1,2] Brian Glancy,[2] Benjamin Bowen,[1] Wayne T. Willis,[2] Zachary Bailowitz,[1] Elena A. De Filippis,[1] Colleen Brophy,[1,3] Christian Meyer,[1] Kurt Højlund,[4] Zhengping Yi,[1,5] and Lawrence J. Mandarino[1,2,6]

OBJECTIVE—The contribution of mitochondrial dysfunction to skeletal muscle insulin resistance remains elusive. Comparative proteomics are being applied to generate new hypotheses in human biology and were applied here to isolated mitochondria to identify novel changes in mitochondrial protein abundance present in insulin-resistant muscle.

RESEARCH DESIGN AND METHODS—Mitochondria were isolated from vastus lateralis muscle from lean and insulin-sensitive individuals and from obese and insulin-resistant individuals who were otherwise healthy. Respiration and reactive oxygen species (ROS) production rates were measured in vitro. Relative abundances of proteins detected by mass spectrometry were determined using a normalized spectral abundance factor method.

RESULTS—NADH- and $FADH_2$-linked maximal respiration rates were similar between lean and obese individuals. Rates of pyruvate and palmitoyl-DL-carnitine (both including malate) ROS production were significantly higher in obesity. Mitochondria from obese individuals maintained higher (more negative) extramitochondrial ATP free energy at low metabolic flux, suggesting that stronger mitochondrial thermodynamic driving forces may underlie the higher ROS production. Tandem mass spectrometry identified protein abundance differences per mitochondrial mass in insulin resistance, including lower abundance of complex I subunits and enzymes involved in the oxidation of branched-chain amino acids (BCAA) and fatty acids (e.g., carnitine palmitoyltransferase 1B).

CONCLUSIONS—We provide data suggesting normal oxidative capacity of mitochondria in insulin-resistant skeletal muscle in parallel with high rates of ROS production. Furthermore, we show specific abundance differences in proteins involved in fat and BCAA oxidation that might contribute to the accumulation of lipid and BCAA frequently associated with the pathogenesis of insulin resistance. ***Diabetes*** **59:2444–2452, 2010**

From the [1]Center for Metabolic Biology, Arizona State University, Tempe, Arizona; the [2]School of Life Sciences, Arizona State University, Tempe, Arizona; the [3]Department of Kinesiology, Arizona State University, Tempe, Arizona; the [4]Harrington Department of Bioengineering, Arizona State University, Tempe, Arizona; the [5]Diabetes Research Centre, Department of Endocrinology, Odense University Hospital, Odense, Denmark; and the [6]Department of Medicine, Mayo Clinic in Arizona, Scottsdale, Arizona.
Corresponding author: Lawrence J. Mandarino, lawrence.mandarino@asu.edu.
Received 5 February 2010 and accepted 15 July 2010. Published ahead of print at http://diabetes.diabetesjournals.org on 3 August 2010. DOI: 10.2337/db10-0174.

Defining the role of mitochondrial dysfunction in the pathogenesis of skeletal muscle insulin resistance has been challenging. If mitochondria were less able to oxidize fatty acids, intramyocellular triacylglycerol and its metabolites, such as long-chain fatty acyl-CoAs, would rise, leading to impaired insulin signaling and insulin resistance (1). Mitochondrial mass is consistently 14–38% lower in muscle in obesity and type 2 diabetes (2–5). In vivo studies, using magnetic resonance spectroscopy, concluded that basal and insulin-stimulated ATP synthesis rates were lower in insulin-resistant offspring of patients with type 2 diabetes (6,7). Although these data suggest intrinsic mitochondrial impairment, it may be that differences in mitochondrial content and cellular ATP demand underlie these observations.

Measurements on isolated mitochondria show that maximal respiration is lower in muscle from type 2 diabetics (8). Studies using saponin-permeabilized isolated human skeletal muscle (SM) fibers reported normal (9) or impaired (10) respiration in type 2 diabetic subjects. Nair et al., in 2009, showed dissociation between insulin sensitivity and mitochondrial ATP synthesis rates while demonstrating an effect of age on isolated mitochondrial activity (11). Given the diversity of these results, the contribution of mitochondrial oxidative capacity to insulin resistance is poorly defined.

Besides an intrinsic impairment in oxidative capacity, increased oxidative stress could produce insulin resistance (12). The superoxide anion ($-O_2\cdot$) is derived from several cellular sources, but the main contributor in SM may be electron leakage from mitochondria (13). At rest, ~0.1–0.2% of consumed oxygen is converted to reactive oxygen species (ROS) (14). Insulin-resistant animal models have higher levels of superoxide production (15), and healthy individuals fed a high-fat diet had increased ROS generation in permeabilized muscle fibers without a change in mitochondrial respiration (16).

This study was undertaken to identify abnormalities in mitochondria isolated from insulin-resistant muscle by assessing mitochondrial bioenergetics and ROS production rates combined with proteomic assessment of abundance of mitochondrial proteins.

RESEARCH DESIGN AND METHODS

Subjects. The purpose, nature and potential risks of the study were explained to the participants, and written consent was obtained. The protocol was approved by the institutional review board of Arizona State University. Additional information is provided in an online appendix (http://diabetes.diabetesjournals.org/cgi/content/full/db10-0174/DC1).

Muscle biopsy and hyperinsulinemic-euglycemic clamp. Participants underwent a euglycemic-hyperinsulinemic clamp with basal muscle biopsies, regarding which the online appendix provides additional information.

Myosin heavy-chain isoform distribution. Myosin heavy-chain (MHC) isoform composition was determined as previously described (17). MHC I, IIx, and IIa protein bands were visualized using Coomasie stain and quantified using densitometry.

Small scale isolation of mitochondria. The online appendix provides information regarding the small-scale isolation of mitochondria.

Mitochondrial energetics. Oxygen uptake by isolated mitochondria was measured using a DW1 Electrode Chamber (Hansatech Instruments, Norfolk, U.K.) in 250 μl respiration medium containing (in millimolar): 100 KCl, 50 3-[N-morpholino] propanesulfonic acid, 10 $K{\cdot}PO_4$, 20 glucose, 10 $MgCl_2$, 1 EGTA, and 0.2% BSA, pH 7.0, at 37°C. Indexes of mitochondrial function were assessed using the following:: 1 mmol/l pyruvate, 10 mmol/l glutamate, 10 μmol/l palmitoyl-DL-carnitine (PC), and 5 mmol/l succinate. All substrates included 1 mmol/l malate to prime the citrate cycle. Mitochondria (10–50 μg) and substrates were added to respiration medium, and maximal (state 3) O_2 consumption rate (JO_2) was stimulated with 125 nmol ADP (0.5 mmol/l). Complete phosphorylation of this ADP bolus elicited transition to resting JO_2 (state 4), which allowed calculation of the ADP-to-O ratio and the state 3–to–state 4 ratio (respiratory control ratio).

Citrate synthase activity. Citrate synthase activity was measured using the method of Srere (18). The online appendix provides further information.

Sensitivity of mitochondria to metabolic control signals. The sensitivity of mitochondrial respiration to kinetic and thermodynamic control signals (free ADP and ATP free energy, respectively) was assessed using the "creatine kinase energy clamp" of Messer et al. (19). Mitochondria (40–60 μg protein) were added to respiration medium containing 1.22 mmol/l phosphocreatine (PCr), 5.0 mmol/l creatine (Cr), and 5.0 mmol/l ATP. Creatine kinase was added in excess (30 units creatine kinase; Sigma Chemical, St. Louis, MO) to maintain thermodynamic equilibrium. Free [ADP] ($[ADP]_f$) was calculated using the equilibrium constant of the creatine kinase reaction (K_{CK}), assumed to be 150 (20):

$$[ADP]_f = ([ATP][Cr])/([PCr]K_{CK})$$

The $[ADP]_f$ with the known phosphate ($[P_i]$) of the medium provided the extramitochondrial free energy of ATP (ΔG_{ATP}): $\Delta G_{ATP} = RT\mathrm{Ln}(\Gamma/K_{ATP})$, where R is the gas constant, T is degrees Kelvin, Γ is the mass action ratio of the ATP hydrolysis reaction ($[ADP]_f[P_i]/[ATP]$), and K_{ATP} is the equilibrium constant of ATP hydrolysis (225,000, based on the study of Teague and Dobson [20]).

Stepwise additions of PCr established progressively lower $[ADP]_f$ and higher (more negative) ΔG_{ATP}, suppressing mitochondrial respiration (supplemental Fig. 1). Eadie-Hofstee analysis of the $[ADP]_f$:JO_2 relation yielded the K_MADP for respiration. Plots of ΔG_{ATP}:JO_2 were near linear (thermodynamic force-flow relation) and were extrapolated through the abscissa to calculate the theoretical ΔG_{ATP} at zero respiration (static head energy) (Fig. 3*A*).

ROS measurement. Substrates (see MITOCHONDRIAL ENERGETICS for concentrations of substrates [10 μmol/l rotenone and 1 μg/μl oligomycin]) were added to respiration medium. Horseradish peroxidase (20 mU) and 10-Acetyl-3,7-dihydroxyphenoxazine (17 ng/μl) were added to a 96-well plate. ROS production was initiated by the addition of 10 μg mitochondrial protein. Optical density was measured every 5 min for 30 min (λex: 550 and λem: 590 nm). Due to limited material, 10 μg rat mitochondria were added to the H_2O_2 standard curve to correct for signal quenching by mitochondria.

Mass spectrometry sample preparation. Forty micrograms of mitochondrial protein were separated by one-dimensional SDS polyacrylamide gel (12%). Proteins were visualized with Coomassie blue (Sigma Chemical, St. Louis, MO). Gel lanes (supplemental Fig. 2) were cut into 20 slices. Each slice was destained, dehydrated, and digested with trypsin as previously described in detail (21). The volume of the extracted peptide solution was reduced to 5 μl by vacuum centrifugation, and 20 μl of 0.1% trifluoroacetic acid/1% formic acid/2% acetonitrile was added.

Mass spectrometry. High-performance liquid chromatography–electrospray ionization–tandem mass spectrometry was performed on a hybrid linear ion trap–Fourier Transform ion cyclotron resonance mass spectrometer (LTQ FT; Thermo Fisher; San Jose, CA) fitted with a PicoView nanospray source (New Objective, Woburn, MA) (refer to Supplemental Information).

TABLE 1
Clinical, metabolic, and skeletal muscle characteristics

	Lean	Obese
N	20	14
Male/female	11/9	7/7
Age (years)	38 ± 3	38 ± 4
BMI (kg/m^2)	25 ± 1	36 ± 1*
Weight (kg)	77.6 ± 3.6	103.1 ± 4.2
Fat mass (kg)	20.4 ± 2.8	37.4 ± 2.5*
Plasma glucose (mg/dl)	86 ± 2	93 ± 2†
Serum insulin (pmol/l)	30 ± 6	90 ± 12*
A1C (%)	5.4 ± 0	5.7 ± 0.1*
HDL cholesterol (mmol/l)	51 ± 3	46 ± 2
LDL cholesterol (mmol/l)	109 ± 9	113 ± 8
Plasma triglycerides (mmol/l)	85 ± 8	126 ± 21†
OGTT (2-h glycemia)	105 ± 6	135 ± 8*
Rd basal (mg · kg^{-1} · min^{-1})	2.1 ± 0.1	1.8 ± 0.1*
Rd clamp (mg · kg^{-1} · min^{-1})	7.9 ± 0.6	3.7 ± 0.3*
HGP clamp (mg · kg^{-1} · min^{-1})	0.1 ± 0.1	0.0 ± 0.1
Pulse (bpm)	67 ± 2	71 ± 2
Systolic/diastolic blood pressure (mmHg)	124 ± 5/82 ± 3	130 ± 3/87 ± 2
Vo_{2max} (ml · min^{-1} · kg^{-1})	31.5 ± 1.9	25.9 ± 1.8
Vo_{2max} (ml · min^{-1} · kg FFM^{-1})	42.9 ± 2.4	38.8 ± 2.0
% MHC I	31 ± 4	24 ± 3
% MHC IIx	21 ± 2	31 ± 4*
% MHC IIa	48 ± 6	45 ± 6
Isolated mitochondrial protein (μg/μl)‡	6.5 ± 0.3	5.4 ± 0.2*
Isolated citrate synthase activity (μmol · min^{-1} · g wet weight^{-1})	8.2 ± 0.6	6.0 ± 0.2*
Mitochondria recovery (%)	66 ± 3	64 ± 3

Data are presented as means ± SE. Student's *t* test was performed. *$P < 0.01$ and †$P < 0.05$ vs. lean participants. ‡Mitochondria pellets were resuspended in 100 μl of mannitol-sucrose buffer. HGP, hepatic glucose production.

Data analysis and bioinformatics. Assignment of individual proteins was completed using Mascot (version 2.2; Matrix Science, London, U.K.) and Scaffold (version 02_00_06; Proteome Software, Portland, OR) as previously described (21) (refer to Supplemental Information).

Normalized spectral abundance factor calculations and immunoblotting. Normalized spectral abundance factors (NSAFs) were calculated for every protein detected in each isolated mitochondria sample as previously described by Hwang et al. (22), who confirmed that this methodology can be applied to complex protein mixtures in a reproducible fashion. In addition, loading 30–120 μg protein lysate generates similar NSAF values (22). Briefly, NSAF values were $\log_2$ transformed to yield a Gaussian distribution. For every protein, the average lean $\log_2$ NSAF values were subtracted from all $\log_2$ NSAF values (both lean and obese groups), resulting in a $\log_2$-fold change for the obese group relative to the lean group. The online appendix provides information regarding immunoblotting.

RESULTS

Metabolic and skeletal muscle characteristics. Lean and obese participants were matched for age, sex, and aerobic capacity (Vo_{2max}) (Table 1). Obese individuals had higher BMI ($P < 0.01$), fasting plasma insulin ($P < 0.01$), A1C ($P < 0.01$), and fasting plasma glucose ($P < 0.05$). Insulin-stimulated glucose disposal was lower in the obese group (7.9 ± 0.6 vs. 3.7 ± 0.3 mg · kg^{-1} · min^{-1}; $P < 0.01$); suppression of endogeneous glucose output was complete in both groups (0.1 ± 0.1 vs. 0.0 ± 0.1 mg · kg^{-1} · min^{-1}). Obese participants had a higher proportion of myosin heavy-chain IIx (*MYHI*) ($P < 0.05$). No differences in MHC

TABLE 2
Respiratory control and ADP-to-O ratios

	Lean	Obese
RCR		
P + M	20.5 ± 1.8	17.4 ± 1.3
PC + M	9.1 ± 1.6	11.4 ± 1.7
P + M + GLU	12.9 ± 2.4	14.1 ± 1.4
GLU + MAL	16.1 ± 1.4	13.7 ± 2.3
P + M + GLU + SUCC	10.0 ± 0.6	10.7 ± 1.2
ADP/O		
P + M	2.30 ± 0.03	2.26 ± 0.05
PC + M	1.94 ± 0.05	1.88 ± 0.06
P + M+ GLU	2.14 ± 0.06	2.03 ± 0.06
GLU + MAL	2.12 ± 0.08	2.02 ± 0.07
P + M + GLU + SUCC	1.77 ± 0.07	1.65 ± 0.03

Data are presented as means ± SE. Lean/obese *n*: pyruvate (P) plus malate (M), 18/12; palmitoyl-DL-carnitine (PC) plus malate, 16/10; pyruvate plus malate plus glutamate (G), 5/11; glutamate plus malate, 7/5; pyruvate plus malate plus glutamate plus succinate (Succ), 7/7.

IIa (*MYH2*) or I (*MYH7*) were observed. Total mitochondrial protein and citrate synthase activity isolated per muscle wet weight were lower in obese individuals ($P < 0.01$), although the proportion of mitochondria recovered in both lean and obese groups was similar (~65%).

In vitro mitochondrial oxidative capacity. ADP-to-O and respiratory control ratios were within previously published ranges for isolated mitochondria from human muscle and did not differ between groups (Table 2). Maximal and resting respiration in response to NADH-linked (pyruvate, malate, and glutamate) and $FADH_2$-linked (succinate) substrates did not differ between the groups (Fig. 1*A* and *B*). PC oxidation also was similar between both groups.

ROS production. Rates of ROS production were measured in the presence of oligomycin in a situation where the ETC complexes were highly reduced by the influx of electrons provided by NADH (pyruvate and PC) and $FADH_2$ (PC). Theoretical sites of ROS production are shown in Fig. 2*A*. With pyruvate and PC (both including malate), insulin-resistant muscle mitochondria produced ROS at higher rates than did insulin-sensitive muscle (Fig. 2*B*). Rotenone addition to inhibit passage of electrons from complex I to ubiquinone typically results in increased ROS production (23). However, rotenone raised ROS production only in the mitochondria from insulin-sensitive individuals.

Mitochondrial sensitivity to metabolic control signals. Steady-state respiration rates spanning the aerobic range were established by experimentally manipulating extramitochondrial energy phosphate levels (ADP) with the creatine kinase energy clamp. Supplemental Fig. 1 shows a typical experiment using stepwise addition of phosphocreatine. Eadie-Hofstee plots of J_{O_2} vs. J_{O_2}/[ADP] yielded similar values for the K_MADP for respiration (35 ± 2 μmol/l for lean vs. 31 ± 4 for obese; $P = 0.33$). Figure 3*A* shows a typical relationship between ΔG_{ATP} and oxygen consumption. The ΔG_{ATP}:J_{O_2} (force flow) relation extrapolated through the abscissa indicated a higher (more negative) static head ΔG_{ATP} in insulin-resistant muscle mitochondria ($P = 0.003$) (Fig. 3*B*). The slope of the force-flow relationship in the lean group showed a trend to be higher than that in the obese group (95.4 ± 7.1 vs. 75.4 ± 8.8 nmol $O_2 \cdot min^{-1} \cdot kcal^{-1} \cdot mol^{-1}$ ($P \leq 0.10$) (supplemental Fig. 3).

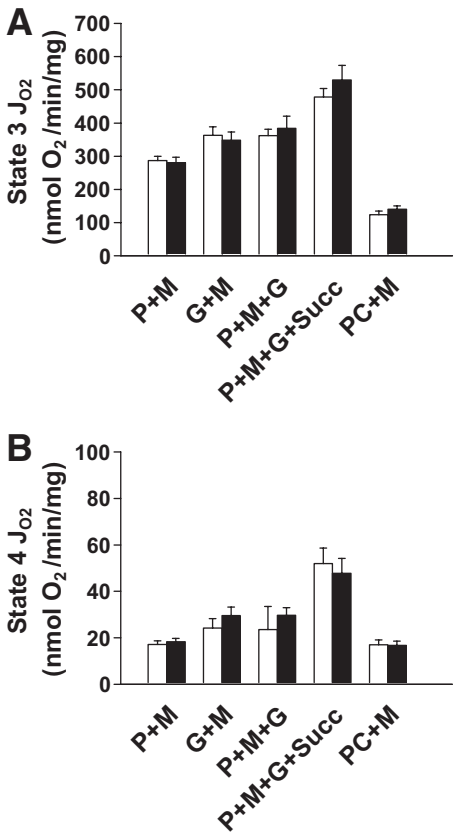

FIG. 1. In vitro oxidative capacity of isolated mitochondria. Mitochondrial fractions were rapidly isolated from basal vastus lateralis biopsies (□, lean insulin-sensitive participants; ■, obese insulin-resistant participants). *A*: State 3 respiration rate was measured in response to 0.5 mmol/l ADP. *B*: State 4 respiration rate was measured following the consumption of 0.5 mmol/l ADP. (See RESEARCH DESIGN AND METHODS for concentrations.) Data are presented as means ± SEM in units of nmol min^{-1} mg $protein^{-1}$. Lean/obese *n*: pyruvate (P) plus malate (M), 18/12; palmitoyl-DL-carnitine (PC) plus malate, 16/10; pyruvate plus malate plus glutamate (G), 5/11; glutamate plus malate, 7/5; pyruvate plus malate plus glutamate plus succinate (Succ), 7/7.

Differences in mitochondrial protein abundance. The number of unique proteins assigned per mitochondrial isolate was similar between the groups (lean 425 ± 19 *v*s. obese 422 ± 29 proteins; P = n.s.), as were the number of total known mitochondrial proteins (lean 248 ± 8 vs. obese 236 ± 13 mitochondrial proteins; P = n.s.). A composite list assigned 691 unique proteins. In addition, the total spectra generated solely by known mitochondrial proteins did not differ between groups (lean 19,683 ± 1,421 vs. obese 18889 ± 1,238; P = n.s.). Approximately 60% of total spectra were assigned to known mitochondrial proteins.

Electron chain complexes. Table 3 depicts the number of assigned subunits in at least half of all participants. Complex II (succinate dehydrogenase) and III (ubiquinone: cytochrome c reductase) subunits were present in equal numbers per mitochondrial mass in insulin-sensitive and insulin-resistant muscle. A number of complex I subunits ($P \leq 0.05$: *NDUFC2*, *NDUFA8*, *NDUFA11*, *NDUFS2*, and *NDUFB8*; $P \leq 0.10$: *NDUFS5*, *NDUFB3*, and *MTND1*) were observed to be lower in abundance in mitochondria from the obese group. The iron-sulfur cluster scaffold protein (*NFU1*) was also lower in the obese group ($P < 0.05$). Only one subunit from complex IV was significantly decreased in obesity: *COX5B* (Table 4).

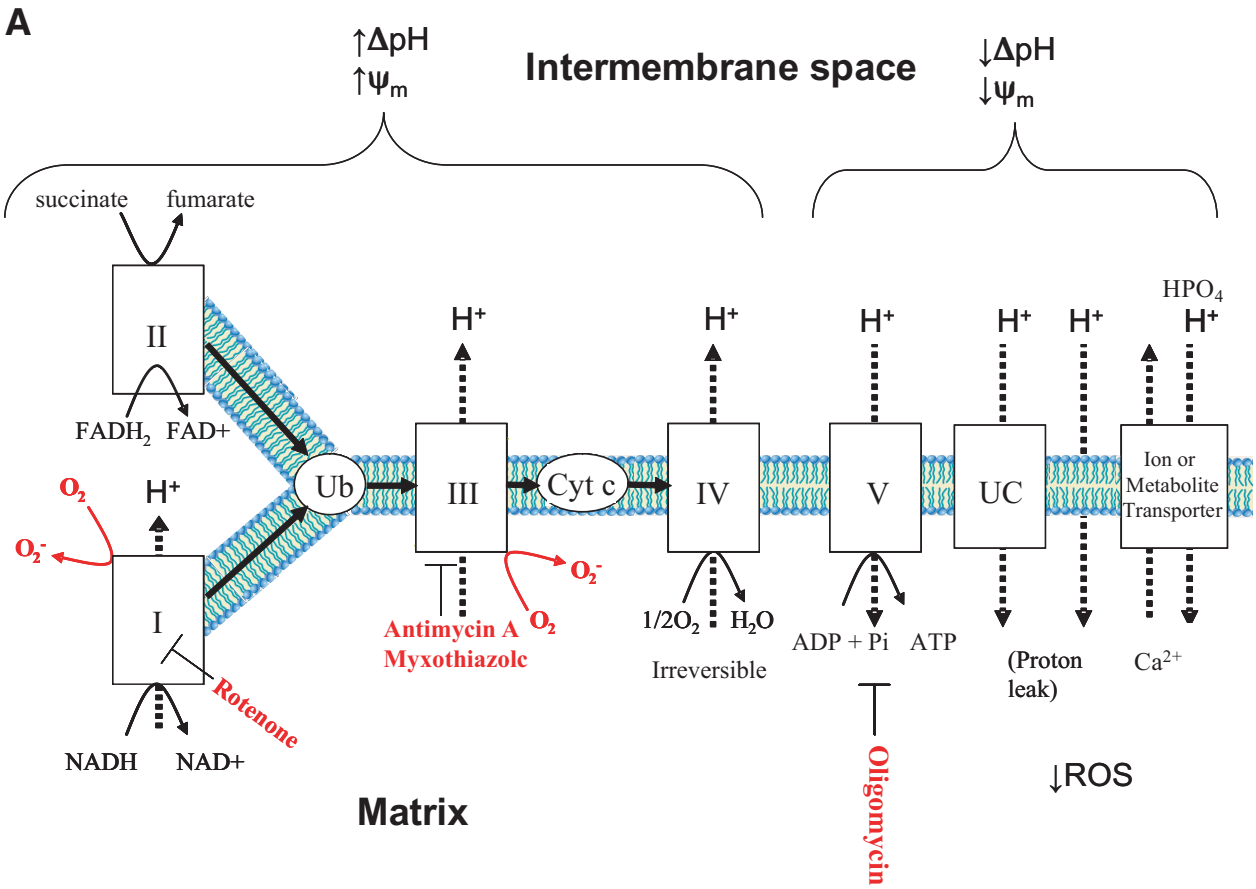

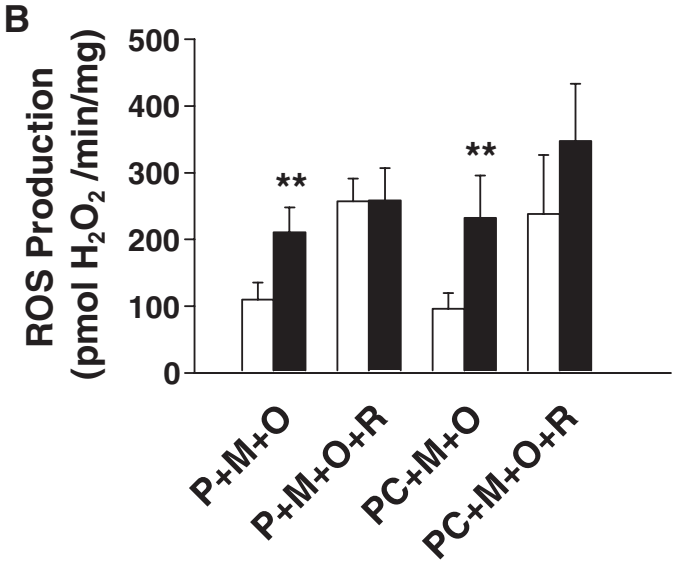

FIG. 2. In vitro ROS production rates. ***A*****: Diagram indicating the electron transport chain complexes along with their substrates (NADH, $FADH_2$, ubiquinone, or cytochrome c) and the inhibitors that target them (red text: rotenone, antimycin A, myxothiazole, and oligomycin). Complexes I and III contain ROS-generating sites (red arrows). Black full arrows show the path of electron flow within the inner mitochondrial membrane (IMM), and black dashed arrows show the directional path of protons across the IMM. Electrons can flow from complex II to I (reverse electron flow) and produce ROS; rotenone blocks this flow from complex II. ROS production by complex I is enhanced in the presence of rotenone because rotenone's binding site is downstream of the ROS-producing site in this complex.** ***B*****: ROS production rates were quantified by incubating isolated mitochondria (10 μg) with various substrate combinations, Amplex Red, and horseradish peroxidase (see RESEARCH DESIGN AND METHODS for detailed procedures). (□, lean insulin-sensitive participants; ■, obese insulin-resistant participants.) Data are presented as means ± SEM;** ***n*** **= 7 per substrate combination. *****P*** **< 0.05 vs. lean participants. G, glutamate; M, malate; O, 1 μg/ml oligomycin; P, pyruvate; PC, palmitoyl-DL-carnitine;** ***R*****, 10 μmol/l rotenone; Succ, succinate.**

Fatty acid oxidation and amino acid metabolism. Carnitine palmitoyltransferase 1B (*CPT1B*) was significantly lower in the obese group. Methyl-malonate-semialdehyde dehydrogenase (*ALDH6A1*) and propionyl-CoA carboxylase β were also lower in mitochondria from the obese group. These proteins are involved in valine and valine/isoleucine oxidation.

Fiber type and related proteins. *MYH2*, coding for myosin type IIa, was higher in the obese versus lean participants; *MYH7* (myosin type I) was unchanged. *MYH1*, coding for myosin type IIx, was higher in the obese participants. In agreement with the myosin isoforms, the Ca^{2+} ATPase fast twitch isoform (*ATP2A1*) was significantly higher and the slow twitch isoform (*ATP2A2*) tended to be lower ($P = 0.07$) in mitochondria from obese individuals. *CASQ2*, the major calsequestrin isoform in cardiac muscle, comprises 50% of the calsequestrin population in slow oxidative muscle fibers. *CASQ2* relative abundance was lower in mitochondria from obese individuals.

Comparison of protein abundance differences identified by mass spectrometry with immunoblot analysis. Mitochondrial lysates were probed for *COXIV* abundance, and no difference was observed between lean and obese

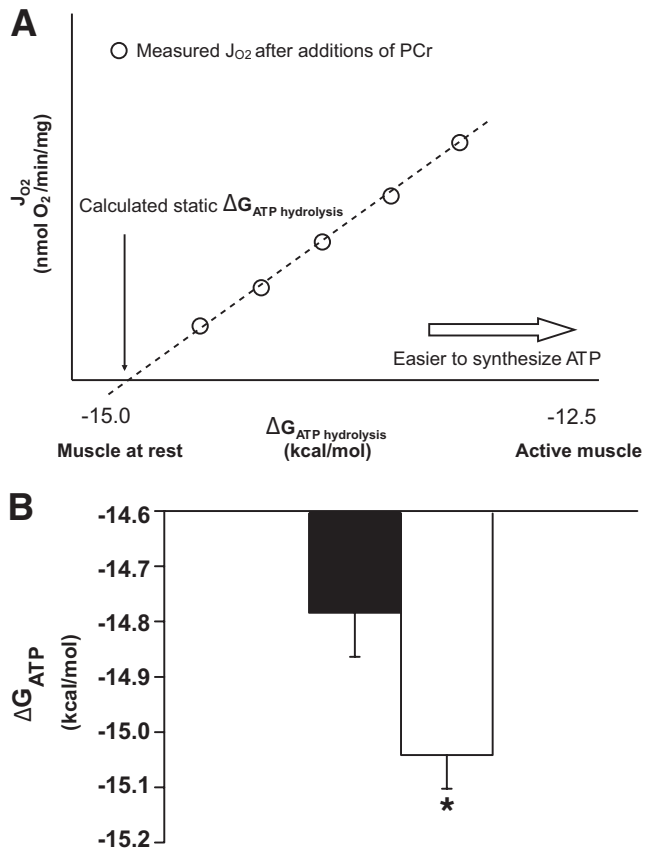

FIG. 3. Static head ΔG_{ATP}. Isolated mitochondria were challenged with pyruvate plus malate at different PCr-to-Cr ratios. *A*: schematic representation of the Jo_2 vs. ΔG_{ATP} plot. *B*: The static head ΔG_{ATP} was calculated by extrapolating the curve of the Jo_2 vs. ΔG_{ATP} curve to Jo_2 = 0. (□, lean insulin-sensitive participants; ■, obese insulin-resistant participants.) Data are presented as means ± SEM; n = 7 per group. Student's t test was performed. *P < 0.01 vs. lean participants.

groups (P = 0.4), as predicted by the mass spectrometry data (Fig. 4). *ALDH6A1* abundance normalized to *COXIV* (P = 0.06) (*ALDH6A1* abundance without normalization to the *COXIV* loading control resulted in P = 0.04) showed a 59% lower abundance in obesity by immunoblot—comparable with the 52% lower abundance determined by mass spectrometry.

DISCUSSION

It has been proposed that excess lipid availability combined with a lower muscular capacity to oxidize fat (24) may lead to accumulation of intramyocellular lipids (25). This in turn is thought to lead to insulin-signaling abnormalities and insulin resistance (1). Lower oxidative capacity could be due to lower mitochondrial content, a defect intrinsic to the individual mitochondrion, or both. Mitochondrial content was significantly lower in the obese individuals, consistent with previous reports (2–5). To determine the presence of intrinsic defects, mitochondria were isolated from lean, insulin-sensitive and obese, insulin-resistant human vastus lateralis muscle. The lower mitochondrial content but similar $V_{O_{2max}}$ values in the obese versus lean volunteers may appear contradictory. However, $V_{O_{2max}}$ primarily reflects cardiovascular, rather than mitochondrial, parameters (26,27).

TABLE 3
Detected ETC subunits by tandem mass spectrometry

Complex	Number of known subunits	Assigned in 16 participants	Assigned in 8 participants
I	46	27	34
II	4	2	2
III	9	5	6
IV	16 (plus SURF1 and SCO1)	7	9
V	19 (plus ATPAF1/2)	10	13

Number of electron transport chain subunits confidently assigned in half or all subjects.

With regard to intrinsic characteristics of the mitochondria, we used the substrate combinations of pyruvate, glutamate, and pyruvate plus glutamate (all including malate), which rely on complex I activity, whereas the addition of succinate recruits complex II activity. Fatty acid oxidation requires complexes I and II and the electron transfer flavoprotein shuttling electrons from dehydrogenases within the β-oxidation pathway to the electron transport chain (ETC). Basal and maximal respiration rates, regardless of substrates, did not differ in the obese participants—a result similar to that in a recent study (11). These findings are in accordance with some (9,28) but not all (8,10) studies assessing mitochondrial function in insulin resistance and type 2 diabetes. Differences between the present results and findings of decreased mitochondrial function in diabetes could be due to the possibility that insulin resistance itself is not associated with gross changes in mitochondrial function or mitochondrial protein abundance; rather, mitochondrial dysfunction may be more associated with hyperglycemia. Results of a whole muscle proteomics comparison of lean and obese normoglycemic and type 2 diabetic individuals showed that decreases in ETC components and other mitochondrial proteins are most pronounced in the diabetics, with more moderate changes in the obese group (22). In addition, most of the earlier studies did not report aerobic fitness measurements (8,9,28), whereas one study did match the control and diabetic subjects for whole-body aerobic power ($V_{O_{2max}}$) (10). The lean and obese individuals in the present study had comparable $V_{O_{2max}}$ and glycemia, and their muscle mitochondria displayed similar maximal substrate oxidation rates, coupling, and respiratory control—in contrast to the study of Phielix et al. (10). These differences suggest that the progression from insulin resistance to type 2 diabetes may result in functional defects in SM mitochondria. On the other hand, our data suggest that reports of decreased in vivo ATP turnover in resting insulin-resistant muscle (6,7,29) most likely reflect decreased cellular ATP demand, given that *1*) in vivo mitochondria rest at <2% of their oxidative potential (30), *2*) the differences in observed mitochondrial content were rather small, and *3*) insulin resistance appears to improve, not degrade, the cellular energy state defended by muscle mitochondria. If higher ΔG_{ATP} had any influence on resting ATP turnover, it would be predicted to be in the opposite direction (31). Our results show that there are no intrinsic defects in mitochondrial oxidative capacity in insulin resistance without hyperglycemia. Taken together, these data indicate that with regard to substrate oxidation, the findings of decreased ATP turnover in vivo (6,7,29) likely are explained on a gross level by a decrease in mitochondrial content in insulin-resistant muscle.

Nevertheless, there were more subtle intrinsic differences in the function of mitochondria from insulin-

TABLE 4
Protein abundance differing significantly in isolated mitochondria from insulin-resistant skeletal muscle of obese subjects

Protein name (gene name)	Fold change in mitochondria from obese (log_2)	P (Student's t test)	Lean/obese subjects with protein assigned (n)	Total spectra per Group	
				Lean	Obese
Myosin-2 (*MYH2*)	0.92 ± 0.16	<0.01	8/8	2,664	4,821
Myosin-1 (*MYH1*)	1.74 ± 0.23	<0.01	8/8	1,691	4,239
Methylmalonate-semialdehyde dehydrogenase [acylating], mitochondrial precursor (*ALDH6A1*)	−1.05 ± 0.12	<0.01	7/5	64	22
Isoform SERCA1A/B of sarcoplasmic/endoplasmic reticulum calcium ATPase 1 (*ATP2A1*)	0.75 ± 0.15	<0.01	8/8	2,433	3,748
Glycogen phosphorylase, muscle form (*PYGM*)	1.40 ± 0.20	<0.01	6/5	19	38
Peroxiredoxin-2 (*PRDX2*)	0.93 ± 0.20	<0.01	8/7	72	113
Prenylcysteine oxidase 1 precursor (*PCYOX1*)	1.07 ± 0.18	0.01	4/6	11	32
Calsequestrin-2 precursor (*CASQ2*)	−0.71 ± 0.11	0.01	8/8	295	169
Dihydropyridine receptor α2 subunit (*CACNA2D1*)	1.17 ± 0.32	0.02	7/7	47	102
Apolipoprotein A-I precursor (*APOA1*)	1.04 ± 0.16	0.02	7/8	56	100
NADH dehydrogenase [ubiquinone] 1 subunit C2 (*NDUFC2*)	−0.58 ± 0.16	0.02	8/8	57	37
Carnitine O-palmitoyltransferase I, muscle isoform (*CPT1B*)	−0.81 ± 0.32	0.03	8/7	114	62
NADH dehydrogenase [ubiquinone] 1α subcomplex subunit 8 (*NDUFA8*)	−0.30 ± 0.12	0.03	8/8	1,487	1,152
NADH dehydrogenase [ubiquinone] 1α subcomplex subunit 11 (*NDUFA11*)	−0.50 ± 0.16	0.04	8/8	259	176
Similar to CG7601-PA (*DHRS7C*)	0.63 ± 0.14	0.04	8/7	64	82
Isoform 1 of tripartite motif-containing protein 72 (*TRIM72*)	−0.85 ± 0.37	0.04	8/6	32	15
Cytochrome c oxidase subunit 5B, mitochondrial precursor (*COX5B*)	−0.33 ± 0.09	0.04	8/8	576	428
NADH dehydrogenase [ubiquinone] iron-sulfur protein 2 (*NDUFS2*)	−0.20 ± 0.05	0.05	8/8	426	349
Propionyl-CoA carboxylase β chain, mitochondrial precursor (*PCCB*)	−0.80 ± 0.21	0.05	5/5	11	6
NADH dehydrogenase;NADH dehydrogenase [ubiquinone] 1β subcomplex subunit 8 (*NDUFB8*)	−0.31 ± 0.13	0.05	8/8	244	188
Erythrocyte band 7 integral membrane protein (*STOM*)	1.24 ± 0.42	0.05	6/8	24	78

Data are means ± SE unless otherwise indicated. Total spectra = sum of spectra across participants within the group.

resistant muscle. In resting muscle, mitochondrial oxidative flux is extremely low (32), with very low $[ADP]_f$ and robust (highly negative) ΔG_{ATP} (31). Contractile activity can elicit extremely high oxidative flux, revealing a cellular aerobic scope spanning two orders of magnitude (30). The metabolic signals that control respiration over this range include both kinetic (e.g., [ADP] or K_MADP) and thermodynamic (ΔG_{ATP}) components. The creatine kinase energy clamp provides an in vitro evaluation of the mitochondrial sensitivity to these signals. In the present study, the K_MADP determined using the creatine kinase clamp for respiration was not different between groups. However, extrapolation of the thermodynamic force-flow relation to the hypothetical zero Jo_2 resulted in significantly more negative (higher) static head ΔG_{ATP} in mitochondria isolated from insulin-resistant muscle. This finding is consistent with the observation of Petersen et al. (6), who used ^{31}P–nuclear magnetic resonance to show that the inorganic phosphate–to–phosphocreatine ratio is lower in insulin-resistant than in insulin-sensitive muscle. Lower inorganic phosphate and more robust ΔG_{ATP} are characteristics that differentiate type II from type I mammalian muscle cells (33). It is therefore noteworthy that insulin-resistant muscle showed trends toward greater expression of type II myocyte proteins, e.g., *MYH2* (type IIa), *MYH1* (type IIx), *ATP2A1* (Ca^{2+} ATPase fast twitch isoform), and higher *PYGM* (glycogen phosphorylase).

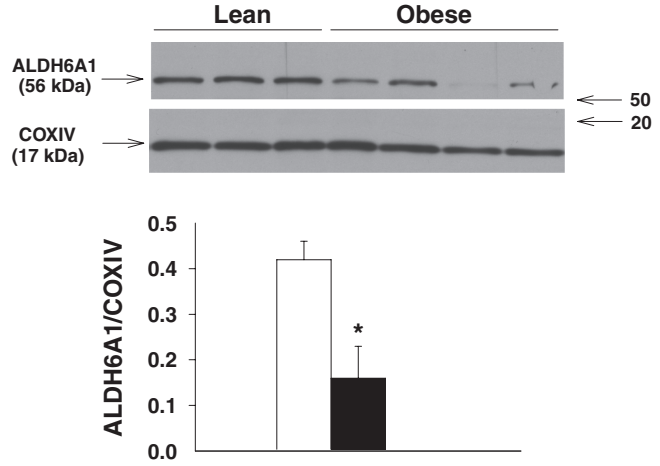

FIG. 4. Comparison of protein abundances determined by mass spectrometry to immunoblotting. Mitochondrial lysates (20 μg) (n = 3–4) were probed for ALDH6A1 and COXIV abundances. ALDH6A1 abundance was normalized to a loading control (COXIV). (□, lean insulin-sensitive participants; ■, obese insulin-resistant participants.) *P = 0.06.

Taken together, these data suggest that, at the low metabolic turnover rates associated with rest, mito-

chondria from insulin-resistant muscle maintain higher thermodynamic driving forces. Because the protonmotive force and the oxidation-reduction energy (redox pressure) down the electron transport chain are the energetic precursors to ΔG_{ATP}, higher ROS production rates by mitochondria from the obese group would be the predicted outcome. This result was experimentally observed. In the absence of rotenone (Fig. 2*A*), ROS production was higher in the obese individuals, suggesting that muscle mitochondria from obese individuals produce more ROS at complex I and/or complex III. Complex III has been labeled as a higher contributor of ROS in SM mitochondria (14). Secondly, the level of long-chain fatty acid oxidation intermediates within the matrix, which have been postulated to be elevated in insulin resistance due to incomplete β-oxidation (34), dictates the amount of ROS produced (35) specifically at the level of complex III and the electron transfer flavoprotein (35). Higher rates of ROS production in insulin resistance have been reported previously (16) and precede the onset of the diabetic state in mice on a high-fat diet (36). Lower rates of ROS production in obese individuals, but not type 2 diabetic individuals, have been reported (37). However, this study did not report maximal ROS production rates because mitochondria were not incubated with oligomycin during the measurements. On the other hand, the insulin-sensitizing effect of exercise training is abrogated upon consumption of antioxidants, supporting a positive role for ROS in the modulation of insulin sensitivity (38). Additionally, mice lacking glutathione peroxidase are protected from insulin resistance induced by high-fat diets (39). Therefore, it is possible that higher ROS production rates observed in isolated mitochondria from obese individuals may be a compensatory mechanism to increase insulin action; this possibility warrants further investigation because ROS have also been identified as a causal factor of insulin resistance (12).

In order to guide future research efforts studying the role of the mitochondrion in insulin resistance, we performed an analysis of the abundance of individual proteins in mitochondria (22,40). We used equal amounts of isolated mitochondrial protein for proteomic analysis, resulting in a comparison of relative protein abundance per mitochondrial mass. Several individual subunits of ETC complex I were significantly reduced in obese, insulin-resistant individuals. Complex I is a 980 kDa conglomerate comprised of 46 subunits in mammals (41). Fourteen of these 46 subunits are the core subunits, responsible for the location of the redox centers (flavin mononucleotide and eight Fe-S cluters) (41). The remaining 32 subunits are less well characterized: they may be involved in maintaining the structure of the complex, in linkage of the complex to the inner mitochondrial membrane, or even in altering ROS generation (41). Five complex I subunits were significantly lower in the obese individuals. These subunits were distributed among the four subcomplexes of complex I (*NDUFB3/B8/C2* in subcomplex Iβ, *ND1* in Iγ, *NDUFA8/A11/S5* in Iα, and *NDUFS2* in Iλ) (41). A negative correlation has previously been found between the degree of insulin resistance and complex I activity (4). *NDUFS2* and *ND1* are two subunits found within the core of complex I. A lower abundance of these two subunits did not translate to a detectable decrease in NADH-linked respiration.

The present study also shows a lower abundance of the muscle outer-mitochondrial membrane carnitine palmitoyltransferase 1B (*CPT1B*). Cpt1B transesterifies long-chain fatty acyl-CoAs to fatty acylcarnitines, which are transported into the mitochondrial matrix for β-oxidation (42). Its expression is dependent on peroxisome proliferator–activated receptor coactivator-1α (PGC-1α) (43) transcription factor activity. Reduced Cpt1B protein level could be a direct consequence of lower PGC-1α gene expression reported in insulin-resistant muscle (44,45). Furthermore, increasing Cpt1B protein levels in SM increased fatty acid oxidation and lowered the severity of insulin resistance in rats on a high-fat diet (46). In the present study, the utilization of PC in the assessment of fatty acid–mediated mitochondrial respiration bypassed the highly regulated CPT system. Our results therefore show that β-oxidation activity per se is not impaired in insulin-resistant muscle but, rather, that the protein determining the rate of fatty acid entry into mitrochondria, Cpt1B, was decreased.

The last set of proteins altered in the proteomics analysis involved enzymes involved in BCAA catabolism. MMS dehydrogenase and propionyl-CoA carboxylase are required for valine and isoleucine metabolism before entry into the tricarboxylic acid (TCA) cycle as succinyl-CoA. Decreased BCAA oxidation, together with increased proteolysis in insulin resistance (47), could lead to increased intracellular BCAA concentrations. Such an increase could activate mammalian target of rapamycin signaling, which can inhibit insulin signaling and produce insulin resistance (48). Moreover, recent metabolomic studies in humans and BCAA/high-fat feeding studies in rodents indicate that alterations in BCAA metabolism are associated with insulin resistance (49,50). Alternatively, or in addition, it is possible that decreased entry of BCAA into the TCA cycle could reduce TCA cycle flux and lead to accumulation of incompletely oxidized fatty acids, as suggested by Koves and Muoio (34). A decreased CPT1B abundance then could be a compensatory effort to protect the cell from accumulation of incompletely oxidized fatty acids and other fatty acid metabolites. A caveat is that this scenario would imply a rate-determining role of BCAA-derived TCA intermediates.

In conclusion, mitochondria isolated from skeletal muscle from obese and overweight insulin-resistant volunteers do not have an intrinsic abnormality in fuel oxidation. However, measurements of citrate synthase activity and mitochondrial protein indicated a decrease in mitochondrial mass. Therefore, in order to maintain similar respiration rates, we propose that mitochondria in insulin-resistant muscle undergo adaptations that allow them to generate a more negative ΔG_{ATP}. A consequence of this higher ΔG_{ATP} would be increased ROS production rates at rest (51) as found here. We propose a model for these data shown in Fig. 5.

We also defined new abnormalities in mitochondria from human insulin-resistant muscle using mass spectrometry. A number of complex I subunits were found to be lower in mitochondria from insulin-resistant muscle, but the lack of characterization of function of most complex I subunits makes it difficult to interpret the consequences of this finding. However, these differences may be related to differences in ROS production. Mitochondria from insulin-resistant muscle also was found to contain less carnitine palmitoyltransferase 1β, offering an explanation for the intramuscular lipid accumulation observed in insulin-resistant muscle (25). In addition, enzymes involved in BCAA

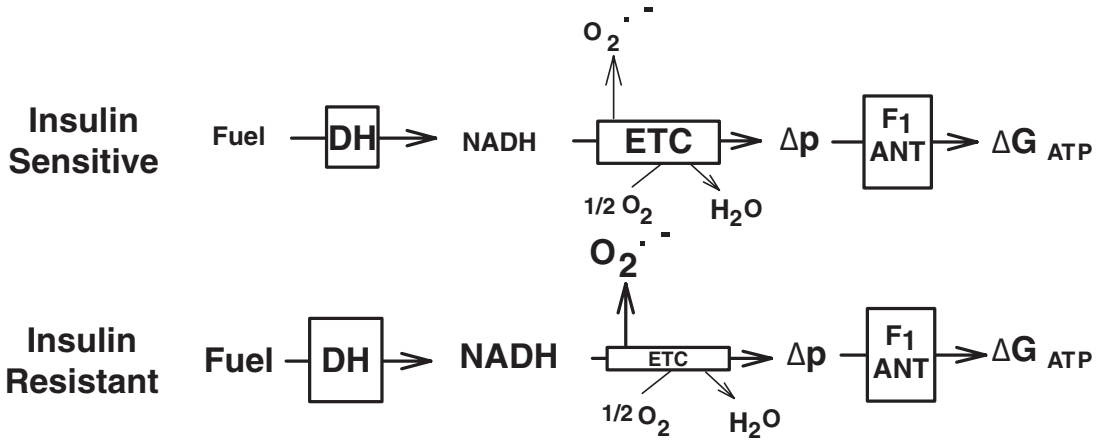

FIG. 5. Proposed bioenergetic model occurring in skeletal muscle insulin resistance. In insulin-resistant skeletal muscle, high catalytic potential in the redox-producing block (i.e., NADH levels) owing to increased citric acid cycle dehydrogenase activity; (isocitrate dehydrogenase [when considering its three subunits] abundance is higher in mitochondria from insulin-resistant muscle [data not shown]) relative to the redox-utilizing block (i.e., ETC, which is particularly impaired by complex I in insulin resistance), which would lead to the following: *1*) higher static head energy (at low flux, high-redox pressure developed by the dehydrogenase is kinetically allowed to achieve near equilibration with ATP energy downstream), *2*) lower ΔG_{ATP}:J_o slope (the impediment to electron flow is exposed by relaxation of downstream ΔG_{ATP} energy and transition to higher flux), and *3*) higher ROS production due to higher driving force (more negative redox potential of electron transfer centers). The protonmotive force (Δp) was not measured and was included for completeness of the model. No differences in the abundance of ATP synthase F1 component or the adenine nucleotide translocator (ANT) were observed in mitochondria from insulin-resistant muscle by mass spectrometry.

metabolism were lower in abundance in insulin-resistant muscle. In addition to the lower mitochondrial content in insulin-resistant muscle, perturbations intrinsic to mitochondria could alter ROS production, limit the entry of fatty acids into the matrix and affect the overall oxidation rate of BCAA.

ACKNOWLEDGMENTS

This study was supported in part by National Institutes of Health grants R01DK47936 (to L.J.M.), R01DK66483 (to L.J.M.), R01DK081750 (to Z.Y.), and the American Diabetes Association.

No potential conflicts of interest relevant to this article were reported.

N.L. researched data, contributed to discussion, wrote the manuscript, and reviewed and edited the manuscript. B.G. researched data. B.B. researched data, contributed to discussion, wrote the manuscript, and reviewed and edited the manuscript. W.T.W. researched data, wrote the manuscript, and reviewed and edited the manuscript. Z.B. researched data. E.A.D.F. researched data. C.B. researched data. C.M. researched data. K.H. researched data. Z.Y. researched data, wrote the manuscript, and reviewed and edited the manuscript. L.J.M. researched data, contributed to discussion, wrote the manuscript, and reviewed and edited the manuscript.

The authors gratefully acknowledge the technical assistance of Kenneth Kirschner, Arizona State University, and the excellent nursing skills of Alexandra Meyer, Julie Robbins, and Dianne Denardo, Arizona State University. The authors are particularly indebted to their enthusiastic participants for willingness to participate in this study.

REFERENCES

1. Szendroedi J, Roden M. Ectopic lipids and organ function. Curr Opin Lipidol 2009;20:50–56
2. Vondra K, Rath R, Bass A, Slabochova Z, Teisinger J, Vitek V. Enzyme activities in quadriceps femoris muscle of obese diabetic male patients. Diabetologia 1977;13:527–529
3. Morino K, Petersen KF, Dufour S, Befroy D, Frattini J, Shatzkes N, Neschen S, White MF, Bilz S, Sono S, Pypaert M, Shulman GI. Reduced mitochondrial density and increased IRS-1 serine phosphorylation in muscle of insulin-resistant offspring of type 2 diabetic parents. J Clin Invest 2005;115:3587–3593
4. Kelley DE, He J, Menshikova EV, Ritov VB. Dysfunction of mitochondria in human skeletal muscle in type 2 diabetes. Diabetes 2002;51:2944–2950
5. Ritov VB, Menshikova EV, He J, Ferrell RE, Goodpaster BH, Kelley DE. Deficiency of subsarcolemmal mitochondria in obesity and type 2 diabetes. Diabetes 2005;54:8–14
6. Petersen KF, Dufour S, Befroy D, Garcia R, Shulman GI. Impaired mitochondrial activity in the insulin-resistant offspring of patients with type 2 diabetes. N Engl J Med 2004;350:664–671
7. Petersen KF, Dufour S, Shulman GI. Decreased insulin-stimulated ATP synthesis and phosphate transport in muscle of insulin-resistant offspring of type 2 diabetic parents. PLoS Med 2005;2:e233
8. Mogensen M, Sahlin K, Fernstrom M, Glintborg D, Vind BF, Beck-Nielsen H, Hojlund K. Mitochondrial respiration is decreased in skeletal muscle of patients with type 2 diabetes. Diabetes 2007;56:1592–1599
9. Boushel R, Gnaiger E, Schjerling P, Skovbro M, Kraunsoe R, Dela F. Patients with type 2 diabetes have normal mitochondrial function in skeletal muscle. Diabetologia 2007;50:790–796
10. Phielix E, Schrauwen-Hinderling VB, Mensink M, Lenaers E, Meex R, Hoeks J, Kooi ME, Moonen-Kornips E, Sels JP, Hesselink MK, Schrauwen P. Lower intrinsic ADP-stimulated mitochondrial respiration underlies in vivo mitochondrial dysfunction in muscle of male type 2 diabetic patients. Diabetes 2008;57:2943–2949
11. Karakelides H, Irving BA, Short KR, O'Brien P, Nair KS: Age, obesity, and sex effects on insulin sensitivity and skeletal muscle mitochondrial function. Diabetes 2009;59:89–97
12. Houstis N, Rosen ED, Lander ES. Reactive oxygen species have a causal role in multiple forms of insulin resistance. Nature 2006;440:944–948
13. Droge W. Free radicals in the physiological control of cell function. Physiol Rev 2002;82:47–95
14. Tahara EB, Navarete FD, Kowaltowski AJ. Tissue-, substrate-, and site-specific characteristics of mitochondrial reactive oxygen species generation. Free Radic Biol Med 2009;46:1283–1297
15. Blendea MC, Jacobs D, Stump CS, McFarlane SI, Ogrin C, Bahtyiar G, Stas S, Kumar P, Sha Q, Ferrario CM, Sowers JR. Abrogation of oxidative stress improves insulin sensitivity in the Ren-2 rat model of tissue angiotensin II overexpression. Am J Physiol Endocrinol Metab 2005;288:E353–E359
16. Anderson EJ, Lustig ME, Boyle KE, Woodlief TL, Kane DA, Lin CT, Price JW 3rd, Kang L, Rabinovitch PS, Szeto HH, Houmard JA, Cortright RN, Wasserman DH, Neufer PD. Mitochondrial H2O2 emission and cellular redox state link excess fat intake to insulin resistance in both rodents and humans. J Clin Invest 2 Feb 2009 [Epub ahead of print]
17. Rockl KS, Hirshman MF, Brandauer J, Fujii N, Witters LA, Goodyear LJ. Skeletal muscle adaptation to exercise training: AMP-activated protein kinase mediates muscle fiber type shift. Diabetes 2007;56:2062–2069
18. Srere PA. Citrate synthase. Methods Enzymol 1969;13:3–5
19. Messer JI, Jackman MR, Willis WT. Pyruvate and citric acid cycle carbon

requirements in isolated skeletal muscle mitochondria. Am J Physiol Cell Physiol 2004;286:C565–C572
20. Teague WE Jr, Dobson GP. Effect of temperature on the creatine kinase equilibrium. J Biol Chem 1992;267:14084–14093
21. Lefort N, Yi Z, Bowen B, Glancy B, De Filippis EA, Mapes R, Hwang H, Flynn CR, Willis WT, Civitarese A, Hojlund K, Mandarino LJ. Proteome profile of functional mitochondria from human skeletal muscle using one-dimensional gel electrophoresis and HPLC-ESI-MS/MS. J Proteomics 2009;72:1046–1060
22. Hwang H, Bowen BP, Lefort N, Flynn CR, De Filippis EA, Roberts C, Smoke CC, Meyer C, Hojlund K, Yi Z, Mandarino LJ. Proteomics analysis of human skeletal muscle reveals novel abnormalities in obesity and type 2 diabetes. Diabetes 2009;59:33–42
23. Liu Y, Fiskum G, Schubert D. Generation of reactive oxygen species by the mitochondrial electron transport chain. J Neurochem 2002;80:780–787
24. Kelley DE, Goodpaster B, Wing RR, Simoneau JA. Skeletal muscle fatty acid metabolism in association with insulin resistance, obesity, and weight loss. Am J Physiol 1999;277:E1130–E1141
25. Goodpaster BH, He J, Watkins S, Kelley DE. Skeletal muscle lipid content and insulin resistance: evidence for a paradox in endurance-trained athletes. J Clin Endocrinol Metab 2001;86:5755–5761
26. Saltin B, Strange S. Maximal oxygen uptake: "old" and "new" arguments for a cardiovascular limitation. Med Sci Sports Exerc 1992;24:30–37
27. Wagner PD. Determinants of maximal oxygen transport and utilization. Annu Rev Physiol 1996;58:21–50
28. Bjorntorp P, Schersten T, Fagerberg SE. Respiration and phosphorylation of mitochondria isolated from the skeletal muscle of diabetic and normal subjects. Diabetologia 1967;3:346–352
29. Befroy DE, Petersen KF, Dufour S, Mason GF, de Graaf RA, Rothman DL, Shulman GI. Impaired mitochondrial substrate oxidation in muscle of insulin-resistant offspring of type 2 diabetic patients. Diabetes 2007;56:1376–1381
30. Richardson RS, Knight DR, Poole DC, Kurdak SS, Hogan MC, Grassi B, Wagner PD. Determinants of maximal exercise VO2 during single leg knee-extensor exercise in humans. Am J Physiol 1995;268:H1453–H1461
31. Jeneson JA, Westerhoff HV, Kushmerick MJ. A metabolic control analysis of kinetic controls in ATP free energy metabolism in contracting skeletal muscle. Am J Physiol Cell Physiol 2000;279:C813–C832
32. Kirkwood SP, Zurlo F, Larson K, Ravussin E. Muscle mitochondrial morphology, body composition, and energy expenditure in sedentary individuals. Am J Physiol 1991;260:E89–E94
33. Kushmerick MJ, Moerland TS, Wiseman RW. Mammalian skeletal muscle fibers distinguished by contents of phosphocreatine, ATP, and Pi. Proc Natl Acad Sci U S A 1992;89:7521–7525
34. Koves TR, Ussher JR, Noland RC, Slentz D, Mosedale M, Ilkayeva O, Bain J, Stevens R, Dyck JR, Newgard CB, Lopaschuk GD, Muoio DM. Mitochondrial overload and incomplete fatty acid oxidation contribute to skeletal muscle insulin resistance. Cell Metab 2008;7:45–56
35. Seifert EL, Estey C, Xuan JY, Harper ME. Electron transport chain-dependent and -independent mechanisms of mitochondrial H2O2 emission during long-chain fatty acid oxidation. J Biol Chem 2009;283:5748–5758
36. Bonnard C, Durand A, Peyrol S, Chanseaume E, Chauvin MA, Morio B, Vidal H, Rieusset J. Mitochondrial dysfunction results from oxidative stress in the skeletal muscle of diet-induced insulin-resistant mice. J Clin Invest 2008;118:789–800
37. Abdul-Ghani MA, Jani R, Chavez A, Molina-Carrion M, Tripathy D, Defronzo RA. Mitochondrial reactive oxygen species generation in obese non-diabetic and type 2 diabetic participants. Diabetologia 2009;52:574–582
38. Ristow M, Zarse K, Oberbach A, Kloting N, Birringer M, Kiehntopf M, Stumvoll M, Kahn CR, Bluher M. Antioxidants prevent health-promoting effects of physical exercise in humans. Proc Natl Acad Sci U S A 2009;106:8665–8670
39. Loh K, Deng H, Fukushima A, Cai X, Boivin B, Galic S, Bruce C, Shields BJ, Skiba B, Ooms LM, Stepto N, Wu B, Mitchell CA, Tonks NK, Watt MJ, Febbraio MA, Crack PJ, Andrikopoulos S, Tiganis T. Reactive oxygen species enhance insulin sensitivity. Cell Metab 2009;10:260–272
40. Lefort N, Yi Z, Bowen B, Glancy B, De Filippis EA, Mapes R, Hwang H, Flynn CR, Willis WT, Civitarese A, Hojlund K, Mandarino LJ. Proteome profile of functional mitochondria from human skeletal muscle using one-dimensional gel electrophoresis and HPLC-ESI-MS/MS. J Proteomics 2009;72:1046–1060
41. Janssen RJ, Nijtmans LG, van den Heuvel LP, Smeitink JA. Mitochondrial complex I: structure, function and pathology. J Inherit Metab Dis 2006;29:499–515
42. Wang D, Harrison W, Buja LM, Elder FF, McMillin JB. Genomic DNA sequence, promoter expression, and chromosomal mapping of rat muscle carnitine palmitoyltransferase I. Genomics 1998;48:314–323
43. Kleiner S, Nguyen-Tran V, Bare O, Huang X, Spiegelman B, Wu Z. PPAR{delta} agonism activates fatty acid oxidation via PGC-1{alpha} but does not increase mitochondrial gene expression and function. J Biol Chem 2009;284:18624–18633
44. Mootha VK, Lindgren CM, Eriksson KF, Subramanian A, Sihag S, Lehar J, Puigserver P, Carlsson E, Ridderstrale M, Laurila E, Houstis N, Daly MJ, Patterson N, Mesirov JP, Golub TR, Tamayo P, Spiegelman B, Lander ES, Hirschhorn JN, Altshuler D, Groop LC. PGC-1alpha-responsive genes involved in oxidative phosphorylation are coordinately downregulated in human diabetes. Nat Genet 2003;34:267–273
45. Patti ME, Butte AJ, Crunkhorn S, Cusi K, Berria R, Kashyap S, Miyazaki Y, Kohane I, Costello M, Saccone R, Landaker EJ, Goldfine AB, Mun E, DeFronzo R, Finlayson J, Kahn CR, Mandarino LJ. Coordinated reduction of genes of oxidative metabolism in humans with insulin resistance and diabetes: Potential role of PGC1 and NRF1. Proc Natl Acad Sci U S A 2003;100:8466–8471
46. Bruce CR, Hoy AJ, Turner N, Watt MJ, Allen TL, Carpenter K, Cooney GJ, Febbraio MA, Kraegen EW. Overexpression of carnitine palmitoyltransferase-1 in skeletal muscle is sufficient to enhance fatty acid oxidation and improve high-fat diet–induced insulin resistance. Diabetes 2009;58:550–558
47. Bell JA, Volpi E, Fujita S, Cadenas JG, Sheffield-Moore M, Rasmussen BB. Skeletal muscle protein anabolic response to increased energy and insulin is preserved in poorly controlled type 2 diabetes. J Nutr 2006;136:1249–1255
48. Tzatsos A, Kandror KV. Nutrients suppress phosphatidylinositol 3-kinase/Akt signaling via raptor-dependent mTOR-mediated insulin receptor substrate 1 phosphorylation. Mol Cell Biol 2006;26:63–76
49. Newgard CB, An J, Bain JR, Muehlbauer MJ, Stevens RD, Lien LF, Ha AM, Shah SH, Arlotto M, Slentz CA, Rochon J, Gallup D, Ilkayeva O, Wenner BR, Yancy WS Jr, Eisenson H, Musante G, Surwit RS, Millington DS, Butler MD, Svetkey LP. A branched-chain amino acid-related metabolic signature that differentiates obese and lean humans and contributes to insulin resistance. Cell Metab 2009;9:311–326
50. Tremblay F, Jacques H, Marette A. Modulation of insulin action by dietary proteins and amino acids: role of the mammalian target of rapamycin nutrient sensing pathway. Curr Opin Clin Nutr Metab Care 2005;8:457–462
51. Korshunov SS, Skulachev VP, Starkov AA. High protonic potential actuates a mechanism of production of reactive oxygen species in mitochondria. FEBS Lett 1997;416:15–18